Rapid Communications

Quantum versus thermal fluctuations in the fcc antiferromagnet: Alternative routes to order by disorder

R. Schick,[1,2] T. Ziman,[1,3] and M. E. Zhitomirsky[2]
[1]*Institut Laue Langevin, 38042 Grenoble Cedex 9, France*
[2]*Université Grenoble Alpes, CEA, IRIG, PHELIQS, 38000 Grenoble, France*
[3]*Université Grenoble Alpes, CNRS, LPMMC, 38000 Grenoble, France*

(Received 20 August 2020; revised 12 November 2020; accepted 23 November 2020; published 9 December 2020)

In frustrated magnetic systems with competing interactions fluctuations can lift the residual accidental degeneracy. We argue that the state selection may have different outcomes for quantum and thermal order by disorder. As an example, we consider the semiclassical Heisenberg fcc antiferromagnet with only the nearest-neighbor interactions. Zero-point oscillations select the type 3 collinear antiferromagnetic state at $T = 0$. Thermal fluctuations favor instead the type 1 antiferromagnetic structure. The opposite tendencies result in a finite-temperature transition between the two collinear states. Competition between effects of quantum and thermal order by disorder is a general phenomenon and is also realized in the J_1-J_2 square-lattice antiferromagnet at the critical point $J_2 = \frac{1}{2}J_1$.

DOI: 10.1103/PhysRevB.102.220405

Introduction. As counterintuitive as it may seem, fluctuations are not always destructive of order, but can actually stabilize broken symmetry states. One prominent example is the isotropic-nematic transition in liquid crystals consisting of hard-rod molecules that, according to Onsager, can be driven entirely by entropy gain in the ordered state [1]. In high-energy physics, vacuum fluctuations are the hallmark of the Coleman-Weinberg mechanism of spontaneous symmetry breakdown in the electrodynamics of massless scalar mesons [2]. The concept of fluctuation-induced ordering has also gained a lot of attention in the field of magnetism. Frustrated magnets with competing interactions often exhibit accidental degeneracy between classical or mean-field ground states that is not dictated by symmetry [3–5]. Their low-temperature behavior and the ultimate ground state selection is sensitive to weak residual interactions but can also be determined solely by fluctuations. In the past, several authors have independently shown that accidental degeneracy in frustrated spin models can be lifted either by quantum or by thermal fluctuations [6–11]. Nowadays, such a fluctuation mechanism is commonly referred to as the effect of order by disorder [12–31].

The early theoretical works have typically found selection of the 'most collinear' states for both quantum ($T = 0$) and classical ($T > 0$) versions of the same frustrated spin model, supporting the perception that the two types of fluctuations play a similar role in the state selection process. Being correct for many weakly frustrated magnets, this assertion is, however, not guaranteed in general; see examples in [22,25,30].

A further limitation of the current picture of thermal order by disorder is that it is mostly based on studies of classical spins. This is, in part, because only the classical Monte Carlo algorithms have proved efficient for frustrated models. The role of thermal fluctuations in quantum spin models attracted much less attention. The available works on this problem [12,17,24] have documented a distinct role of thermal fluctuations for a few specific spin models, but generality of the obtained results remain unclear.

The difference between quantum and thermal order by disorder is easily recognized by considering two standard expressions. At $T = 0$, the zero-point (vacuum) energy is given by

$$E_0 = \frac{1}{2}\sum_{\mathbf{k}} \epsilon_{\mathbf{k}}, \tag{1}$$

where $\epsilon_{\mathbf{k}}$ are energies of bosonic magnon modes. At the same time, their free energy is ($k_B = 1$)

$$\Delta F = T\sum_{\mathbf{k}} \ln(1 - e^{-\epsilon_{\mathbf{k}}/T}). \tag{2}$$

Both types of fluctuations favor states with soft excitations, but the "softness" criterion appears to be different in each case. Minimization of the zero-point energy (1) picks the states with the smallest average magnon energy. Thermal fluctuations (2) instead select states with the largest density of low-energy excitations $\epsilon_{\mathbf{k}} \sim T$. In frustrated magnets the low-energy excitations include the pristine Goldstone modes determined by the broken symmetry and the so-called pseudo-Goldstone modes. The latter appear due to an accidental degeneracy of the classical ground states and have a distinct structure for each of the ground states. Since the two selection mechanisms rely on magnons with different energies, their outcomes can also vary.

The thermal effects vanish as $T \to 0$, hence, a natural question is whether the thermal contribution (2) can overcome the zero-temperature splitting (1). In our paper we demonstrate that the semiclassical Heisenberg antiferro-

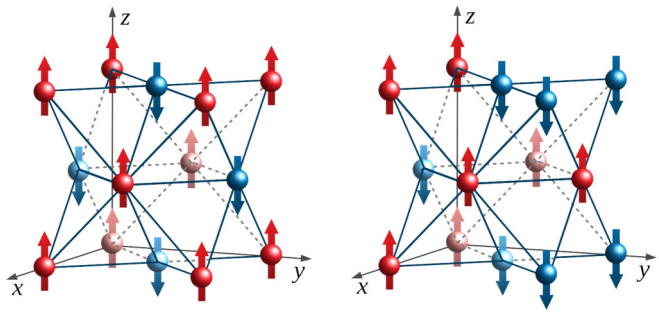

FIG. 1. Type 1 (left) and type 3 (right) antiferromagnetic structures on an fcc lattice.

magnet (AFM) on a face-centered cubic (fcc) lattice with nearest-neighbor interactions exhibits a finite-temperature transition within magnetically ordered state determined by competition between the two fluctuation mechanisms. A competition between thermal and quantum order by disorder effects is also predicted for the frustrated square-lattice antiferromagnet showing that such a behavior is ubiquitous among frustrated models.

FCC antiferromagnet, $T = 0$. The Heisenberg AFM on an fcc lattice is one of the oldest frustrated spin models [32–37]. It keeps attracting significant interest because of numerous experimental realizations [38–45]. We consider the Heisenberg model with spins of length S and the nearest-neighbor exchanges of strength J:

$$\mathcal{H} = J \sum_{\langle ij \rangle} \mathbf{S}_i \cdot \mathbf{S}_j. \tag{3}$$

Each spin couples to 12 nearest neighbors located at $(0, \pm a/2, \pm a/2)$, $(\pm a/2, 0, \pm a/2)$, $(\pm a/2, \pm a/2, 0)$, where a is the linear size of a cubic cell.

The lowest-energy classical states of (3) are coplanar spin spirals with the propagation vectors belonging to the line

$$\mathbf{Q}_s = \frac{2\pi}{a}(1, q, 0) \tag{4}$$

and other equivalent directions in the cubic Brillouin zone. Their classical energy $E_{cl} = -2JS^2$ does not depend on the pitch parameter q. For each degeneracy line there are two special commensurate wave vectors

$$\mathbf{Q}_1 = \frac{2\pi}{a}(1, 0, 0) \quad \text{and} \quad \mathbf{Q}_3 = \frac{2\pi}{a}\left(1, \frac{1}{2}, 0\right) \tag{5}$$

that accommodate collinear states called respectively the type 1 (AF1) and type 3 antiferromagnetic (AF3) structures; see Fig. 1. The two collinear states become unique ground states in the presence of a weak second-neighbor exchange either of FM (type 1) or AFM (type 3) sign [36]. This makes them natural candidates for the order by disorder selection in the nearest-neighbor case [46].

Significant efforts were previously devoted to investigation of thermal order by disorder for the classical fcc antiferromagnet [46–51]. Large-scale Monte Carlo simulations clearly demonstrated the presence of the AF1 state below the first-order transition at $T_c \approx 0.446JS^2$ [51]. Surprisingly, the quantum selection for the Heisenberg fcc antiferromagnet (3) was not addressed in detail apart from one early work [34], which came, as is shown below, to an incorrect conclusion. The main focus of more recent theoretical studies [52–62] was on the effect of further-neighbor exchanges, anisotropies, etc.

We consider semiclassical spins $S \gg 1$ and use the linear spin-wave theory (LSWT) to study the ground state selection by quantum fluctuations. Spin operators are bosonized via the Holstein-Primakoff transformation applied in the rotating local frame and only quadratic terms in boson operators are kept. The quadratic form is diagonalized by the Bogolyubov transformation, allowing one to compute the magnon dispersion $\epsilon_{\mathbf{k}}$ and the ground-state energy per spin

$$E_{\text{g.s.}} = -2JS(S+1) + \frac{1}{2}\sum_{\mathbf{k}} \epsilon_{\mathbf{k}}, \tag{6}$$

where summation is taken over the first Brillouin zone. All steps are completely standard—see, e.g., [63]—and below we present only the final expressions.

For an arbitrary spin spiral on the degeneracy line (4) the magnon energy is

$$\epsilon_{s\mathbf{k}} = 4JS\,[1 + c_x c_y + c_x c_z + c_y c_z]^{1/2} \times [1 - c_x c_z + c_y(c_z - c_x)\cos(\pi q)]^{1/2}. \tag{7}$$

To simplify formulas we define $c_\alpha = \cos(k_\alpha a/2)$, $s_\alpha = \sin(k_\alpha a/2)$ for $\alpha = x, y, z$. The excitation spectrum for the AF1 state is obtained by taking $q \to 0$ in the above equation:

$$\epsilon_{1\mathbf{k}} = 4JS\sqrt{s_x^2(c_y + c_z)^2 + s_y^2 s_z^2}. \tag{8}$$

For $q = 1/2$, Eq. (7) describes magnons in the noncollinear spiral state with the propagation vector $\mathbf{Q}_3$ and 90° angle between neighboring spins. The spectrum of the collinear AF3 state cannot be described in a simple rotating basis. One has to include two sites in the unit cell and introduce two types of bosons. Accordingly, there are two magnon modes for each wave vector,

$$\left(\frac{\epsilon^{\pm}_{3\mathbf{k}}}{4JS}\right)^2 = 1 - c_x^2 c_z^2 \pm \left[c_y^2(c_x + c_z)^2(1 - c_x c_z)^2 + s_y^4\left(c_x^2 - c_z^2\right)^2 + s_x^2 s_y^2 s_z^2 (c_x - c_z)^2\right]^{1/2}, \tag{9}$$

which both contribute to the zero-point energy, but the momentum summation is now performed over half of the Brillouin zone. The dispersion relation (9) was previously derived by Swendsen [37]. However, the early work by ter Haar and Lines [34,35] gave $\epsilon_{\mathbf{k}}$ equivalent to Eq. (7) with $q = 1/2$, which applies to the $\mathbf{Q}_3$ spiral rather than to the collinear AF3 state [64]. The magnon dispersion in the collinear states is illustrated in Fig. 2. Apart from the normal Goldstone modes at the momenta $\mathbf{k} = 0$ and $\mathbf{k} = \mathbf{Q}_1$ or $\mathbf{Q}_3$ the excitation spectra contain the line nodes that appear due to the classical degeneracy.

The zero-point energy for degenerate classical ground states has been computed numerically using the magnon spectra (7)–(9). Results quoted below contain all significant digits. Combining E_0 with the state-independent negative shift, Eq. (6), we obtain for the ground-state energy of the

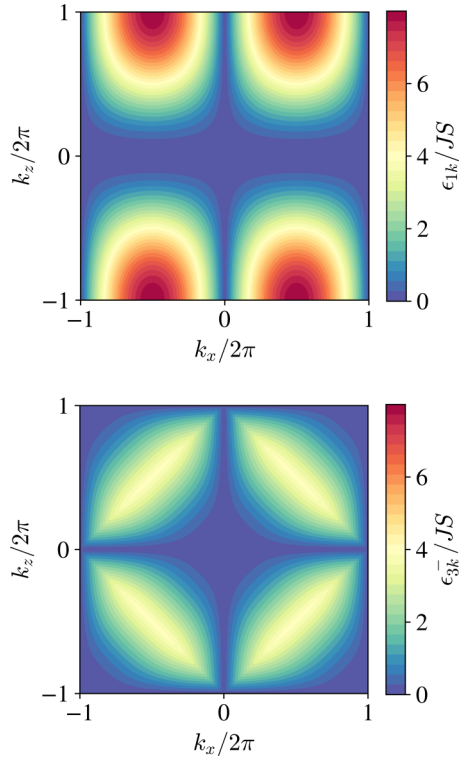

FIG. 2. Color intensity map for the magnon dispersion in two collinear antiferromagnetic states with fixed $k_y = 2\pi/a$: AF1 (top panel) and AF3, lower branch (bottom panel).

AF1 state

$$E^{(1)}_{\text{g.s.}} = E_{cl}\left(1 + \frac{0.488056}{2S}\right), \tag{10}$$

where $E_{cl} = -2JS^2$. The first three digits of the $1/S$ correction agree with the result of Ref. [52]. For the AF3 structure the integration yields

$$E^{(3)}_{\text{g.s.}} = E_{cl}\left(1 + \frac{0.491106}{2S}\right), \tag{11}$$

which is lower than $E^{(1)}_{\text{g.s.}}$. The inset of Fig. 3 shows the quantum energy correction $\Delta E = E^{(s)}_{\text{g.s.}} - E_{cl}$ for the spin spirals (4), which is always above $\Delta E^{(1)}$ [64]. Thus, at variance with [34] we find that the LSWT gives the lowest energy for the AF3 state albeit with a rather small energy difference $\Delta E_0 \approx 0.003JS$. This conclusion is further supported by the numerical exact-diagonalization study of the spin-1/2 model [65], which found enhanced spin-spin correlations at the wave vector $\mathbf{Q}_3$ in comparison to $\mathbf{Q}_1$. Still, a small size of the employed cluster ($N = 32$) prevents us from making any definite statement about the state selection in the $S = 1/2$ case. Therefore, it will be interesting to check how the higher-order spin-wave corrections modify the ground-state energies of the AF1 and AF3 spin structures.

We conclude the $T = 0$ case with results for the ordered moments. Due to the additional pseudo-Goldstone modes the spin reduction $\Delta S = S - \langle S \rangle$ is substantial for both states:

$$\Delta S_1 = 0.338\,75, \quad \Delta S_3 = 0.366\,30. \tag{12}$$

In agreement with the fluctuation mechanism, the lowest energy state exhibits a larger spin reduction.

FCC antiferromagnet, finite T. The free energy (2) has been computed in the low-temperature region $T \ll JS^2$ using the bare magnon spectra. We normalize temperature to JS and drop the classical energy, which leaves the same JS scaling for both contributions (1) and (2). Figure 3 shows the total free energy $F = E_0 + \Delta F$ for the two collinear states. Remarkably, curves cross at $T^* \approx 0.21JS$, indicating the first-order transition into the AF1 state above T^*. This is an interesting example of competition between thermal and quantum order by disorder. Clearly, the transition is possible because of a small initial difference in the zero point energies of the competing states.

To further understand the thermal vs quantum competition, we derive analytically the low-temperature asymptotes for $\Delta F(T)$ in the two states. Let us begin with the AF1 structure. The energy (8) has two types of line nodes: (i) L_x line $\mathbf{k} = (k_x, 2\pi/a, 0)$ and (ii) L_z line $\mathbf{k} = (0, 2\pi/a, k_z)$. All other zero-energy excitations fall in one of the above categories. The difference between L_x and L_z nodes is prominent already from Fig. 1. The small momentum expansion around the L_x line gives

$$\epsilon_{1\mathbf{k}} \approx JSa^2\sqrt{k_y^2k_z^2 + \tfrac{1}{4}s_x^2\left(k_y^2 - k_z^2\right)^2} \simeq k_\perp^2, \tag{13}$$

whereas for the L_z line $\epsilon_{1\mathbf{k}} \simeq k_\perp$. The softer L_x magnons dominate at low temperatures and yield the power law asymptote

$$\Delta F_1 \propto -T^2 \tag{14}$$

and $C \propto T$ behavior of the specific heat. These should be contrasted with a much weaker thermal effect $\Delta F \propto -T^4$ ($C \propto T^3$) in nonfrustrated 3D antiferromagnets.

The magnon dispersion for the AF3 state also has line nodes, but they have a linear dispersion and play only a secondary role. The dominant contribution

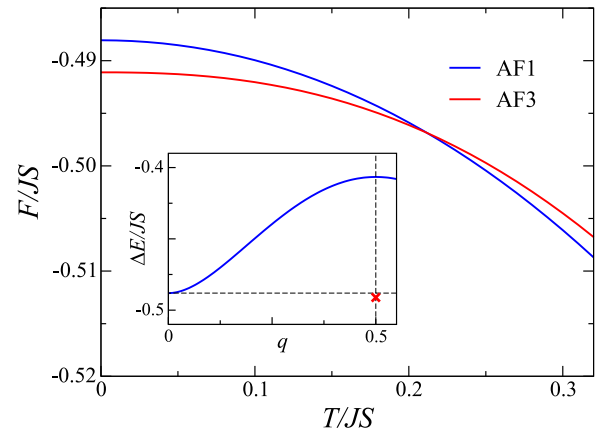

FIG. 3. Main panel: temperature dependence of the free energy in the AF1 and AF3 states. Inset: the quantum correction ΔE to the ground-state energy for the degenerate classical spirals vs pitch q (full line). ΔE for the AF3 state is marked with a cross.

into ΔF_3 comes from the crossing points of such lines; see Fig. 1. In the vicinity of the crossing point $(0, 2\pi/a, 0)$ the lowest magnon branch (9) is anomalously soft,

$$\epsilon^{-}_{3\mathbf{k}} \approx \frac{JSa^2}{\sqrt{2}}\sqrt{k_y^2\left(k_x^2+k_z^2\right)+\tfrac{1}{16}\,k_x^2k_z^2\left(k_x^2+k_z^2\right)}, \tag{15}$$

where both the leading and the subleading terms are necessary for deriving the correct asymptote. A lengthy analytic calculation gives in this case

$$\Delta F_3 \propto -T^{7/3}. \tag{16}$$

The two power laws (14) and (16) fully agree with the numerical results in Fig. 3. Thus, the different thermal response in the two states is determined by a different structure of the pseudo-Goldstone modes.

Generally, the higher-order $1/S$ corrections renormalize the harmonic spectrum and induce a small quantum gap $\Delta_g = O(1/S)$ for the pseudo-Goldstone modes. Such calculations have been carried out before in a few simple cases [31,53,66,67]. The normal three-dimensional behavior $\Delta F \propto -T^4$ is recovered at ultralow temperatures $T \ll \Delta_g$, leaving almost intact the T dependences (14) and (16) in the intermediate regime $\Delta_g \ll T \lesssim JS$. Note that the nonlinear effects also remove the divergent finite-T contribution to the sublattice magnetization, which was regarded as an indication of the absence of a long-range order at finite temperatures in the fcc antiferromagnet [33,34].

The predicted transition at $T^* \approx 0.21JS$ occurs away from the classical regime $T \sim JS^2$, where a large-S model behaves essentially as a classical spin system. Hence, the thermal order by disorder effect discussed here is not directly related to the similar selection in the classical model. Indeed, the harmonic excitation spectra are identical for the classical AF1 and AF3 states and the thermal selection relies on the nonlinear processes [51].

Frustrated square-lattice antiferromagnet. We now briefly consider the Heisenberg J_1-J_2 antiferromagnet on a square lattice (FSAFM); for a review see [68]. Depending on the ratio of two exchanges the model has the following classical ground states: the Néel state with $\mathbf{Q} = (\pi, \pi)$ for $J_2/J_1 \leqslant 1/2$ and the stripe state with $\mathbf{Q} = (\pi, 0)$ or $\mathbf{Q} = (0, \pi)$ for $J_2/J_1 \geqslant 1/2$. We focus on the critical point $J_2/J_1 = 1/2$, where the classical degeneracy of FSAFM is reminiscent of the fcc antiferromagnet. Apart from the two degenerate collinear states, there is an infinite number of spin spirals of equal energy with $\mathbf{Q} = (\pi, q)$ and $\mathbf{Q} = (q, \pi)$.

We perform the LSWT calculations at $J_2/J_1 = 1/2$ in the two collinear states of FSAFM [69], and obtain the magnon dispersion in the Néel state as

$$\epsilon_{\mathbf{k}} = 2J_1S|\sin k_x||\sin k_y|, \tag{17}$$

whereas in the stripe phase [$\mathbf{Q} = (\pi, 0)$] the dispersion is

$$\epsilon_{\mathbf{k}} = 2J_1S|\sin k_x|(1+\cos k_y). \tag{18}$$

The excitation spectra possess the line nodes in accordance with the classical degeneracy, but the asymptotic behavior of $\epsilon_{\mathbf{k}}$ in their vicinity is markedly different between the two states. An elementary integration yields for the zero-point energy

$$E_0^{\text{Neel}} = \frac{4}{\pi^2}J_1S < E_0^{\text{stripe}} = \frac{2}{\pi}J_1S, \tag{19}$$

with the Néel state having a lower energy because of a more narrow magnon bandwidth. Thus, at $J_2 = \frac{1}{2}J_1$, the quantum fluctuations stabilize the Néel state in full agreement with the numerical evaluation of two spin-wave contributions [70].

At low temperatures the leading contributions to the free energy are also straightforwardly computed as

$$\Delta F^{\text{Neel}} = -T^2\ln T, \quad \Delta F^{\text{stripe}} = -T^{3/2}. \tag{20}$$

The stripe phase is favored by the thermal fluctuations due to its softer pseudo-Goldstone modes ($\epsilon_{\mathbf{k}} \sim k_y^2$). Hence, FSAFM provides another example of the thermal-quantum competition, though a finite-temperature transition (crossover) between the two competing state is precluded due to a fairly large energy difference $\Delta E_0 \approx 0.23J_1S$ at zero T. It will be interesting to check how the interlayer coupling present in possible experimental realizations of FSAFM affect this competition.

Conclusions. The difficulties in the spin-wave theory for the fcc antiferromagnet were recognized more than half a century ago [33], but not really resolved. By making a full linear spin-wave analysis of the Heisenberg model we have elucidated a number of interesting points: we find a qualitative difference between the effects of quantum corrections and thermal excitations and predict a phase transition between two collinear states, each favored by specific type of fluctuations. We relate the differences to the structure of zero-frequency (pseudo-Goldstone) magnons that are responsible for the anomalous power laws in the free energy as a function of temperature. These should be visible in the temperature dependence of the specific heat and may serve as an experimental hint of order by disorder in real materials. A similar transition due to competing order by disorder effects has been found for the Heisenberg-Kitaev model on a hyper-honeycomb lattice [24], though the role played by pseudo-Goldstone modes was not investigated.

The obtained results are valid for the fcc antiferromagnets with large spins $S \gg 1$. For small spins, the higher-order quantum corrections may become important and it is necessary to investigate their effect both analytically and numerically.

Competition between quantum and thermal order by disorder must be ubiquitous among frustrated magnets. The primary candidates are spin systems with degeneracy along lines in the momentum space similar to the fcc and FSAFM models considered here. Such spiral degeneracy naturally appears from the frustrating further-neighbor Heisenberg exchanges [71,72]. It can also arise from anisotropic nearest-neighbor interactions on geometrically frustrated lattices [23,27,62]. We hope that the presented results will stimulate further interest in the role of thermal fluctuations in quantum frustrated models.

Note added in proof. Recently, D. Kriese *et al.* [73] presented numerical FRG results that favor the AF3 state in the spin-1/2 fcc AFM at zero temperature, in agreement with our conclusion.

Acknowledgments. We thank Y. Iqbal, P. Grigoriev, and J. Villain for helpful discussions. M.E.Z. acknowledges financial support from ANR, France (Grant No. ANR-18-CE05-0023). T.Z. thanks the JAEA, Tokai, Japan for support under the Reimei program "New materials for spintronics assessed by quantum beams".

[1] L. Onsager, Ann. N.Y. Acad. Sci. **51**, 627 (1949).
[2] S. Coleman and E. Weinberg, Phys. Rev. D **7**, 1888 (1973).
[3] E. F. Shender and P. C. W. Holdsworth, in *Fluctuations and Order*, edited by M. Millonas (Springer, Berlin, 1995).
[4] R. Moessner, Can. J. Phys. **79**, 1283 (2001).
[5] *Introduction to Frustrated Magnetism*, edited by C. Lacroix, P. Mendels, and F. Mila (Springer, Berlin, 2011).
[6] J. R. Tessman, Phys. Rev. **96**, 1192 (1954).
[7] E. Belorizky, R. Casalegno, and J. Niez, Phys. Status Solidi B **77**, 495 (1976).
[8] J. Villain, R. Bidaux, J.-P. Carton, and R. Conte, J. Phys. (Paris) **41**, 1263 (1980).
[9] E. F. Shender, Zh. Eksp. Teor. Fiz. **83**, 326 (1982) [Sov. Phys. JETP **56**, 178 (1982)].
[10] E. Rastelli, L. Reatto, and A. Tassi, J. Phys. C **16**, L331 (1983).
[11] H. Kawamura, J. Phys. Soc. Jpn. **53**, 2452 (1984).
[12] E. Rastelli and A. Tassi, J. Phys. C: Solid State Phys. **21**, L35 (1988).
[13] C. L. Henley, Phys. Rev. Lett. **62**, 2056 (1989).
[14] P. Chandra, P. Coleman, and A. I. Larkin, Phys. Rev. Lett. **64**, 88 (1990).
[15] A. V. Chubukov and D. I. Golosov, J. Phys.: Condens. Matter **3**, 69 (1991).
[16] J. T. Chalker, P. C. W. Holdsworth, and E. F. Shender, Phys. Rev. Lett. **68**, 855 (1992).
[17] Q. Sheng and C. L. Henley, J. Phys.: Condens. Matter **4**, 2937 (1992).
[18] T. Yildirim, A. B. Harris, and E. F. Shender, Phys. Rev. B **53**, 6455 (1996).
[19] R. Moessner and J. T. Chalker, Phys. Rev. B **58**, 12049 (1998).
[20] M. E. Zhitomirsky, A. Honecker, and O. A. Petrenko, Phys. Rev. Lett. **85**, 3269 (2000).
[21] D. Bergman, J. Alicea, E. Gull, S. Trebst, and L. Balents, Nat. Phys. **3**, 487 (2007).
[22] J.-S. Bernier, M. J. Lawler, and Y. B. Kim, Phys. Rev. Lett. **101**, 047201 (2008).
[23] M. E. Zhitomirsky, M. V. Gvozdikova, P. C. W. Holdsworth, and R. Moessner, Phys. Rev. Lett. **109**, 077204 (2012).
[24] S. B. Lee, E. K.-H. Lee, A. Paramekanti, and Y. B. Kim, Phys. Rev. B **89**, 014424 (2014).
[25] A. L. Chernyshev and M. E. Zhitomirsky, Phys. Rev. Lett. **113**, 237202 (2014).
[26] B. Javanparast, A. G. R. Day, Z. Hao, and M. J. P. Gingras, Phys. Rev. B **91**, 174424 (2015).
[27] G. Jackeli and A. Avella, Phys. Rev. B **92**, 184416 (2015).
[28] I. Rousochatzakis, J. Reuther, R. Thomale, S. Rachel, and N. B. Perkins, Phys. Rev. X **5**, 041035 (2015).
[29] J. G. Rau, S. Petit, and M. J. P. Gingras, Phys. Rev. B **93**, 184408 (2016).
[30] B. Danu, G. Nambiar, and R. Ganesh, Phys. Rev. B **94**, 094438 (2016).
[31] J. G. Rau, P. A. McClarty, and R. Moessner, Phys. Rev. Lett. **121**, 237201 (2018).
[32] P. W. Anderson, Phys. Rev. **79**, 705 (1950).
[33] J. M. Ziman, Proc. Phys. Soc. A **66**, 89 (1953).
[34] D. ter Haar and M. E. Lines, Phil. Trans. R. Soc. Lond. A **255**, 1 (1962).
[35] M. E. Lines, Proc. R. Soc. London A **271**, 105 (1963).
[36] Y. Yamamoto and T. Nagamiya, J. Phys. Soc. Jpn. **32**, 1248 (1972).
[37] R. H. Swendsen, J. Phys. C **6**, 3763 (1973)
[38] M. S. Seehra and T. M. Giebultowicz, Phys. Rev. B **38**, 11898 (1988).
[39] M. Matsuura, Y. Endoh, H. Hiraka, K. Yamada, A. S. Mishchenko, N. Nagaosa, and I. V. Solovyev, Phys. Rev. B **68**, 094409 (2003).
[40] A. L. Goodwin, M. T. Dove, M. G. Tucker, and D. A. Keen, Phys. Rev. B **75**, 075423 (2007).
[41] A. M. Balagurov, I. A. Bobrikov, S. V. Sumnikov, V. Yu. Yushankhai, and N. Mironova-Ulmane, JETP Lett. **104**, 88 (2016).
[42] A. A. Aczel, A. M. Cook, T. J. Williams, S. Calder, A. D. Christianson, G.-X. Cao, D. Mandrus, Y.-B. Kim, and A. Paramekanti, Phys. Rev. B **93**, 214426 (2016).
[43] T. Chatterji, L. P. Regnault, S. Ghosh. and A. Singh, J. Phys.: Condens. Matter **31**, 125802 (2019).
[44] N. Khan, D. Prishchenko, Y. Skourski, V. G. Mazurenko, and A. A. Tsirlin, Phys. Rev. B **99**, 144425 (2019).
[45] A. Revelli, C. C. Loo, D. Kiese, P. Becker, T. Frohlich, T. Lorenz, M. Moretti Sala, G. Monaco, F. L. Buessen, J. Attig, M. Hermanns, S. V. Streltsov, D. I. Khomskii, J. van den Brink, M. Braden, P. H. M. van Loosdrecht, S. Trebst, A. Paramekanti, and M. Gruninger, Phys. Rev. B **100**, 085139 (2019).
[46] C. L. Henley, J. Appl. Phys. **61**, 3962 (1987).
[47] J. F. Fernández, H. A. Farach, C. P. Poole, and M. Puma, Phys. Rev. B **27**, 4274 (1983).
[48] W. Minor and T. M. Giebultowicz, J. Phys. Colloq. **49**, C8-1551 (1988).
[49] H. T. Diep and H. Kawamura, Phys. Rev. B **40**, 7019 (1989).
[50] J. L. Alonso, A. Tarancón, H. G. Ballesteros, L. A. Fernández, V. Martín-Mayor, and A. Muñoz Sudupe, Phys. Rev. B **53**, 2537 (1996).
[51] M. V. Gvozdikova and M. E. Zhitomirsky, JETP Lett. **81**, 236 (2005).
[52] T. Oguchi, H. Nishimori, and T. Taguchi, J. Phys. Soc. Jpn. **54**, 4494 (1985).
[53] T. Yildirim, A. B. Harris, and E. F. Shender, Phys. Rev. B **58**, 3144 (1998).
[54] R. S. Fishman and S. H. Liu, Phys. Rev. B **58**, R5912 (1998).
[55] J.-P. Ader, Phys. Rev. B **65**, 014411 (2001).
[56] A. N. Ignatenko, A. A. Katanin, and V. Y. Irkhin, JETP Lett. **87**, 555 (2008).
[57] T. Datta and D.-X. Yao, Phys. Rev. B **85**, 054409 (2012).
[58] H. Ishizuka and L. Balents, Phys. Rev. B **92**, 020411(R) (2015).

[59] P. Sinkovicz, G. Szirmai, and K. Penc, Phys. Rev. B **93**, 075137 (2016).
[60] L. A. Batalov and A. V. Syromyatnikov, J. Magn. Magn. Mater. **414**, 180 (2016).
[61] A. Singh, S. Mohapatra, T. Ziman, and T. Chatterji, J. Appl. Phys. **121**, 073903 (2017).
[62] F.-Y. Li, Y.-D. Li, Y. Yu, A. Paramekanti, and G. Chen, Phys. Rev. B **95**, 085132 (2017).
[63] M. E. Zhitomirsky and I. A. Zaliznyak, Phys. Rev. B **53**, 3428 (1996).
[64] See Eqs. (3.4)–(3.6) in [35]. Figure 4 of [34] gives the energy difference between the AF1 and AF3 states at the Heisenberg point ($J_\gamma = 0$) the same as in the inset of our Fig. 3 between the AF1 and the spiral state with $\mathbf{Q}_3$ ($q = 0.5$).
[65] K. Lefmann and C. Rischel, Eur. Phys. J. B **21**, 313 (2001).
[66] G. Khaliullin, Phys. Rev. B **64**, 212405 (2001).
[67] M. Holt, O. P. Sushkov, D. Stanek, and G. S. Uhrig, Phys. Rev. B **83**, 144528 (2011).
[68] B. Schmidt and P. Thalmeier, Phys. Rep. **703**, 1 (2017).
[69] C. Bruder and F. Mila, Europhys. Lett. **17**, 463 (1992).
[70] G. Jackeli and M. E. Zhitomirsky, Phys. Rev. Lett. **93**, 017201 (2004).
[71] E. Rastelli, A. Tassi, and L. Reatto, Physica B **97**, 1 (1979).
[72] N. Niggemann, M. Hering, and J. Reuther, J. Phys.: Condens. Matter **32**, 024001 (2020).
[73] D. Kiese, T. Mueller, Y. Iqbal, R. Thomale, and S. Trebst, arXiv:2011.01269.